Immunity
Article

Interferon-γ-Responsive Nonhematopoietic Cells Regulate the Immune Response to *Mycobacterium tuberculosis*

Ludovic Desvignes[1] and Joel D. Ernst[1,2,3,*]
[1]Division of Infectious Diseases, Department of Medicine
[2]Department of Pathology
[3]Department of Microbiology
New York University School of Medicine, 550 First Avenue, Smilow 901, New York, NY 10016, USA
*Correspondence: joel.ernst@med.nyu.edu
DOI 10.1016/j.immuni.2009.10.007

SUMMARY

Immunity to *Mycobacterium tuberculosis* in humans and in mice requires interferon gamma (IFN-γ). Whereas IFN-γ has been studied extensively for its effects on macrophages in tuberculosis, we determined that protective immunity to tuberculosis also requires IFN-γ-responsive nonhematopoietic cells. Bone marrow chimeric mice with IFN-γ-unresponsive lung epithelial and endothelial cells exhibited earlier mortality and higher bacterial burdens than control mice, underexpressed indoleamine-2,3-dioxygenase (*Ido1*) in lung endothelium and epithelium, and overexpressed interleukin-17 (IL-17) with massive neutrophilic inflammation in the lungs. We also found that the products of IDO catabolism of tryptophan selectively inhibit IL-17 production by Th17 cells, by inhibiting the action of IL-23. These results reveal a previously unsuspected role for IFN-γ responsiveness in nonhematopoietic cells in regulation of immunity to *M. tuberculosis* and illustrate the role of IDO in the inhibition of Th17 cell responses.

INTRODUCTION

Interferon gamma (IFN-γ) is essential to restrict progressive, fatal infection with *Mycobacterium tuberculosis*. Patients that are either deficient in IFN-γ (Fieschi et al., 2003) or are incapable of responding to IFN-γ because of mutations in IFN-γR1 or IFN-γR2 suffer severe tuberculosis (Jouanguy et al., 1997), as well as infections with less virulent species of mycobacteria (Filipe-Santos et al., 2006). Likewise, IFN-γ-deficient mice infected with *M. tuberculosis* die rapidly with high bacterial burdens in the lungs (Cooper et al., 1993; Flynn et al., 1993), implying that IFN-γ contributes to the restriction of bacterial growth. Efforts to understand the actions of IFN-γ that contribute to restriction and/or killing of *M. tuberculosis* have been confined to studies of macrophages because these cells are known to harbor the bacteria in vivo and because IFN-γ was originally characterized as a macrophage-activating factor (Nathan, 1983). Subsequent studies have revealed essential roles for IFN-γ-responsive genes such as *Nos2* (MacMicking et al., 1997) and *Irgm1* (MacMicking et al., 2003), which provide nonoverlapping functions that restrict *M. tuberculosis* in cultured macrophages and in mice. In addition, IFN-γ treatment of cultured macrophages has been shown to promote acidification of mycobacterial phagosomes (Schaible et al., 1998) and autophagy, which can result in limited intracellular killing of *M. tuberculosis* (Gutierrez et al., 2004). Whereas these studies have advanced our knowledge of the roles of IFN-γ in the control of tuberculosis by immune cells, a comprehensive understanding of the contribution of IFN-γ to immunity to *M. tuberculosis* is still lacking.

Because *M. tuberculosis* infection of cultured macrophages inhibits IFN-γ induction of selected genes (Banaiee et al., 2006; Nagabhushanam et al., 2003; Ting et al., 1999), and because IFN-γR and the molecules of the JAK-STAT pathway, required for IFN-γ signaling, are expressed in diverse cell types, including nonhematopoietic cells such as epithelial and endothelial cells and fibroblasts (Schroder et al., 2004), we hypothesized that control of *M. tuberculosis* also requires responses to IFN-γ by nonhematopoietic cells. To test this hypothesis, we used IFN-γR1-deficient and wild-type mice to prepare bone marrow chimeric mice whose hematopoietic and nonhematopoietic cells were selectively incapable of responding to IFN-γ. We confirmed that early control of *M. tuberculosis* infection requires IFN-γ-responsive hematopoietic cells; we found that long-term control of tuberculosis also requires IFN-γ-responsive nonhematopoietic cells. In the absence of IFN-γR1 on nonhematopoietic cells, mice succumbed to *M. tuberculosis* infection, with severe inflammation in the lungs. Expression of IFN-γ-responsive genes and immunohistochemical analyses revealed that IFN-γR1-deficient nonhematopoietic cells under-expressed indoleamine-2,3-dioxygenase in lung epithelium and endothelium during chronic tuberculosis, and this was accompanied by overexpression of IL-17 and massive recruitment of neutrophils to the lungs. These results extend the previously published observation that control of an intracellular pathogen requires IFN-γ-responsive hematopoietic and nonhematopoietic cells when the pathogen invades both cell types (e.g., *Toxoplasma gondii*) (Yap and Sher, 1999). We thus showed that IFN-γ-responsive nonhematopoietic cells are also required for control of *M. tuberculosis*, which, unlike *T. gondii*, resides predominantly, if not exclusively, in hematopoietic cells such as macrophages, dendritic cells, and neutrophils (Wolf et al., 2007).

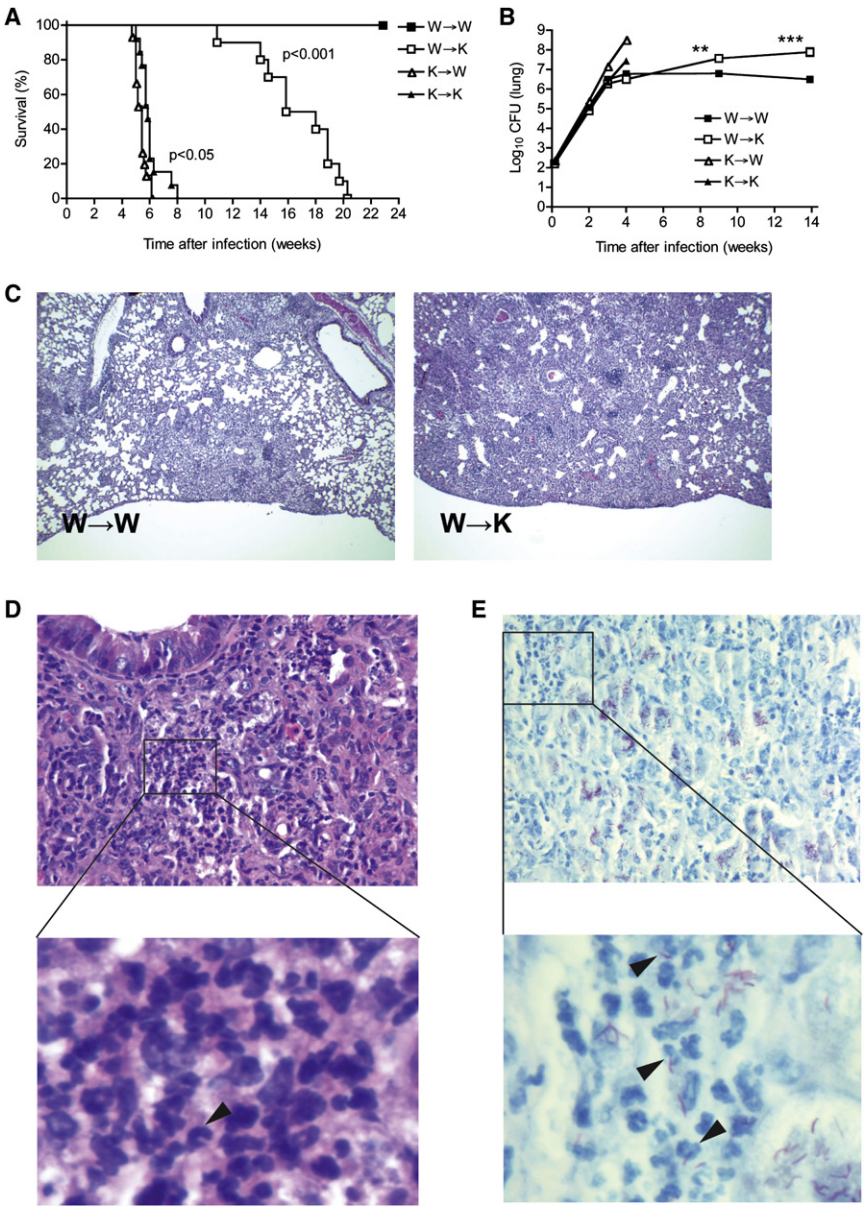


Figure 1. Control of Long-Term *M. tuberculosis* Infection Is Impaired in the Absence of IFN-γR1 on Nonhematopoietic Cells

(A) Survival of chimeric mice after infection with *M. tuberculosis*: W→W (n = 5), W→K (n = 15), K→W (n = 15), and K→K (n = 10). Data are representative of three independent experiments. Groups were compared with a log rank test.

(B) Bacterial load in the lungs of infected chimeric mice as evaluated by plating serial dilutions of lung homogenates on 7H11 agar. Data are representative of three independent experiments and expressed as the mean (±SE) of four mice per time point and per group. Groups were compared with unpaired Student's t test with a 95% confidence interval. **p < 0.01, ***p < 0.005. Bacterial loads in the lungs of the respective groups of chimeric mice 3 and 4 weeks postinfection are presented in Figure S2A.

(C) Lung histopathology in W→W and W→K mice 14 weeks after infection with *M. tuberculosis*. Lung left lobes were fixed in paraformaldehyde for a minimum of 7 days. Histopathology was analyzed by hematoxylin and eosin (H&E) staining of paraformaldehyde-fixed paraffin-embedded 5 mm tissue sections 14 weeks after aerosol infection with M. tuberculosis. The image is shown at 40× the original magnification.

(D) Neutrophils (arrowhead) infiltrating the lungs of W→K mice as evidenced by H&E staining 14 weeks post-infection. The image is shown at 400× the original magnification. The inset is shown at 1000× magnification.

(E) Kinyoun's acid-fast staining with brilliant green counterstaining showing neutrophils infected with *M. tuberculosis* (arrowheads) in the lungs of W→K mice 14 weeks after infection. The image is shown at 400× the original magnification. The inset is shown at 1000× magnification.

Taken together, these findings illustrate the contribution of parenchymal cells in regulation of immune responses, especially in the context of infection with persistent pathogens such as *M. tuberculosis*.

RESULTS

Immune Control of Tuberculosis Requires IFN-γ-Responsive Nonhematopoietic Cells

To test the hypothesis that IFN-γ contributes to immune control of tuberculosis by effects on cells other than macrophages, we examined the consequences of the absence of IFN-γ responsiveness in hematopoietic versus nonhematopoietic cells on survival and pathology after a low-dose aerosol infection of mice with *M. tuberculosis*.

We found that chimeric mice reconstituted with *Ifngr1*$^{-/-}$ bone marrow cells died soon after infection, regardless of the presence of IFN-γR1 on nonhematopoietic cells (Figure 1A). Remarkably, wild-type mice reconstituted with *Ifngr1*$^{-/-}$ bone marrow (K→W mice) died significantly earlier than *Ifngr1*$^{-/-}$ mice reconstituted with *Ifngr1*$^{-/-}$ bone marrow (K→K mice) (median survival = 5.4 ± 0.2 weeks versus 5.9 ± 0.3 weeks, $p < 0.05$; Figure 1A). The earlier death of K→W mice was accompanied by higher bacterial burdens in the lungs than in K→K mice as measured 3 weeks (6.4 ± 0.1 versus 7.2 ± 0.1 $\log_{10}$; $p = 0.0018$; Figure 1B and Figure S2A available online) and 4 weeks postinfection (8.5 ± 0.1 versus 7.4 ± 0.2 $\log_{10}$; $p = 0.0014$; Figure 1B and Figure S2A). The gross lung pathology of K→W mice was also the most severe at that time (Figure S3A) and, although the lesions appeared less extensive at the histological level than in K→K mice, they were more multifocal (Figure S3C). These results provide evidence that when hematopoietic cells, including macrophages, are incapable of responding to IFN-γ, the response of nonhematopoietic cells to IFN-γ is actually

detrimental, as manifest by poorer control of bacterial growth in the lungs. Our observations in K→K and K→W mice also substantiate the long-held belief that macrophages need to respond to IFN-γ in order to control infection with *M. tuberculosis*.

In contrast to the mice whose hematopoietic cells were incapable of responding to IFN-γ, mice whose nonhematopoietic cells were *Ifngr1*$^{-/-}$ (W→K mice) survived the acute phase of the infection (Figure 1A). They were no less capable of arresting progressive growth of *M. tuberculosis* in the lungs 4 weeks after infection than were mice with wild-type hematopoietic and nonhematopoietic cells (W→W mice) (Figure 1B). In fact, they had significantly fewer bacteria in their lungs at week 3 ($p = 0.0445$) and week 4 ($p = 0.012$) (Figure S2A). Both groups also displayed small pulmonary lesions at that time (Figure S3). However, the W→K mice succumbed earlier than the W→W mice during the chronic phase of infection (median survival = 16.9 ± 1.1 weeks versus 27 ± 0.6 weeks, $p < 0.001$). All uninfected bone marrow chimeric mice survived for over 30 weeks, indicating that death of the infected W→K mice was due to *M. tuberculosis*. To assess the cause of death of the W→K mice, we examined their ability to control growth of *M. tuberculosis* and found that as the infection progressed beyond its fourth week, *M. tuberculosis* continued to grow in the lungs of W→K mice while the bacterial burden was maintained at a plateau in W→W mice (Figure 1B). Consequently, the lung bacterial load in W→K mice surpassed that in W→W mice and by 14 weeks, as the mice of this group began to succumb, the number of mycobacteria in the lungs reached 7.9 ± 0.2 $\log_{10}$, 1.4 $\log_{10}$ higher than in W→W mice at the same time ($p < 0.001$). The W→K mice also had significantly higher bacterial loads in the mediastinal lymph node ($p < 0.01$) (Figure S2B) and the spleen ($p < 0.01$) (Figure S2C) on week 14 postinfection. Gross pathologic examination of the lungs showed that W→W mice had numerous focal subpleural lesions, whereas W→K mice displayed no surface lesions (Figure S3B). Microscopic examination revealed organized cellular aggregates limited to the peripheral areas of the lungs in W→W mice, whereas the entire pulmonary tissue of W→K mice was diffusely affected, with a marked increase in cellularity (Figure 1C). Dense infiltrates of polymorphonuclear granulocytes, most likely neutrophils, were observed in the lungs of W→K mice (Figure 1D). In some areas of the lungs, neutrophils and *M. tuberculosis* could be visualized in close association (Figure 1E). Together, these observations indicate that the response to IFN-γ in nonhematopoietic cells plays an essential role in the control of *M. tuberculosis* growth in the lungs after the acute phase of the infection.

Cell Recruitment to the Lungs of IFN-γR Bone Marrow Chimeras Infected with *M. tuberculosis*

To determine whether the susceptibility of W→K mice was due to defective activation and/or recruitment of immune cells to the site of infection, we examined the cell populations in the lungs during the course of infection.

The total number of cells did not differ significantly ($p > 0.05$) between W→W and W→K mice for up to 9 weeks of infection with *M. tuberculosis* (Figure 2A). During this phase, the number of leukocytes in the lungs increased sharply in both groups, peaked at 4 weeks postinfection then decreased progressively until week 9. After week 9, the total number of cells remained unchanged in the lungs of W→W mice but increased significantly ($p = 0.0499$) in W→K mice. Analysis of the T cell populations in the lungs of chimeric mice during infection revealed no significant difference ($p > 0.05$) in CD4$^+$ or CD8$^+$ T cells between the two groups of mice (Figure S4A). In both groups of mice, the population of CD4$^+$ T cells increased sharply after infection,

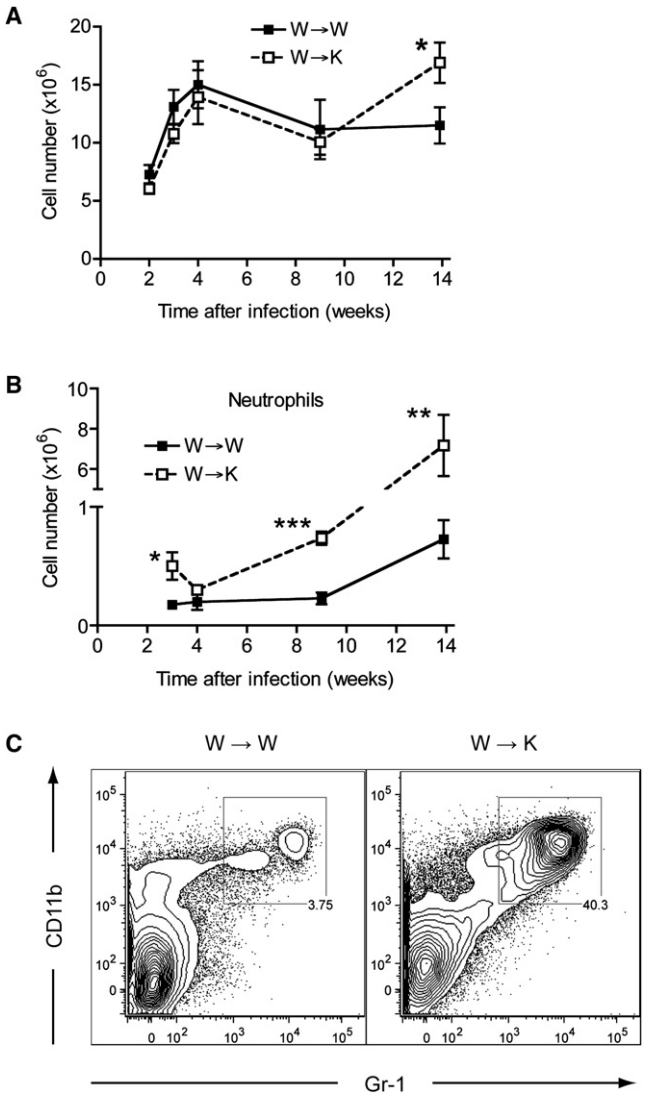


Figure 2. Cell Populations in the Lungs of IFN-γR Chimeric Mice during *M. tuberculosis* Infection

(A) Total cell number in the lungs and their viability were assessed on single-cell suspensions obtained from infected chimeric mice. Viability was higher than 90%. Results are expressed as the mean number (±SE) of total cells per lung and for four mice per time point and per group. Data were compared with a two-tailed Student's t test, *$p < 0.05$.

(B) Recruitment of neutrophils to the lungs of W→W and W→K mice during infection with *M. tuberculosis*. Neutrophils were quantitated by flow cytometry with single-cell suspensions stained with anti-CD11b and anti-Gr1. Results are expressed as the average number (±SE) of CD11b^{hi}Gr1^{hi} cells per lung and for four mice per time point and per group. Data were compared using a two-tailed Student's t test, *$p < 0.05$, **$p < 0.01$, and ***$p < 0.005$.

(C) Representative dot plots showing the proportion of CD11b^{hi}Gr1^{hi} cells in W→W and W→K mice 14 weeks after infection with *M. tuberculosis*.

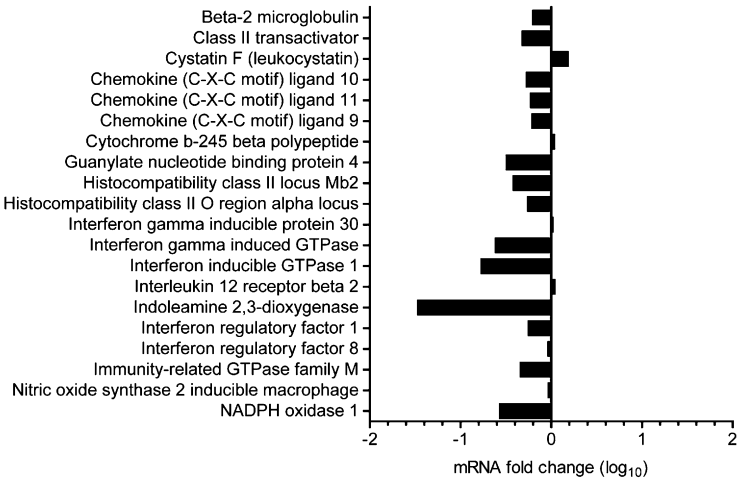


Figure 3. Differential Expression of IFN-γ-Responsive Genes in the Lungs of Chimeric Mice Infected with *M. tuberculosis* for 9 Weeks

Microarray analysis was conducted on pools of RNA isolated from four mice per group and the pools of each group were hybridized against each other. The results are expressed as the fold change in mRNA expression in W→K mice over W→W mice.

peaking at 4 weeks then contracting to a plateau during the chronic phase of infection. The number of $CD8^+$ T cells also increased upon *M. tuberculosis* infection, peaked at 4 weeks, but experienced a smaller decline, without any plateau. As we have previously reported (Wolf et al., 2008), $CD4^+$ and $CD8^+$ T cells also increased in number in the mediastinal (lung-draining) lymph node after infection; there was no significant difference ($p > 0.05$) in T cell expansion in the lymph node between W→W and W→K mice (data not shown).

We (Wolf et al., 2007) and others (Gonzalez-Juarrero et al., 2003; Skold and Behar, 2008) have shown that *M. tuberculosis* induces the recruitment of several subsets of myeloid cells to the lungs. When we compared populations of myeloid cells in the lungs of *M. tuberculosis*-infected mice, we found that those of W→K mice contained significantly ($p < 0.05$) fewer $CD11c^{hi}CD11b^{hi}$ myeloid dendritic cells and $CD11c^{lo}CD11b^{hi}$ inflammatory, interstitial macrophages during the early stages of infection when compared to the lungs of W→W mice (Figure S4B). The differences between the two groups of mice diminished in the later stages of infection, when these myeloid populations contracted in the W→W mice. There was no significant difference ($p > 0.05$) between the two experimental groups in the populations of $CD11c^{hi}CD11b^{lo}$ alveolar macrophages and $CD11c^{-}CD11b^{hi}Gr\text{-}1^{-}$ monocytes. During the acute phase of infection, $CD11b^{hi}Gr\text{-}1^{hi}$ granulocytes were more abundant in lungs of W→K mice than in W→W mice (week 3: $5.0 \pm 1.2 \times 10^5$ versus $1.8 \pm 0.1 \times 10^5$ cells, $p = 0.031$), but by week 4, this population contracted to the same level as in wild-type mice (Figure 2B). At later time points, flow cytometry analysis confirmed the microscopic findings (Figures 1D and 1E): $CD11b^{hi}Gr\text{-}1^{hi}$ neutrophils were recruited to the lungs in large numbers. By week 9, the abundance of granulocytes rose sharply in the lungs of W→K mice, whereas it remained unchanged in W→W mice (Figure 2B). At week 14, ~2 weeks prior to the average time of death, W→K mice had ~30% more cells in their lungs than W→W mice ($1.6 \pm 0.17 \times 10^7$ versus $1.2 \pm 0.17 \times 10^7$ cells, $p < 0.05$), and $CD11b^{hi}Gr\text{-}1^{hi}$ neutrophils fully accounted for this increase (Figures 2B and 2C). These results show that nonhematopoietic cells contribute to the IFN-γ-dependent recruitment of myeloid cells to the lungs during *M. tuberculosis* infection.

Differential Gene Expression in the Lungs of IFN-γR Chimeric Mice during *M. tuberculosis* Infection

To further understand the mechanisms underlying the immune response to *M. tuberculosis* in W→K mice, we compared gene expression profiles in the lungs by using microarray analysis. We first focused our attention on well-characterized IFN-γ-responsive genes (Ehrt et al., 2001; Sana et al., 2005). During the chronic phase of infection, of the 20 IFN-γ-responsive genes that we selected and analyzed by microarray, 12 were not differentially expressed between the two experimental groups (i.e., less than 2-fold difference) and seven genes were significantly but moderately (more than 2-fold but less than 10-fold difference) underexpressed in the lungs of W→K mice in comparison to those of W→W mice (Figure 3). Indoleamine 2,3-dioxygenase (*Ido1*) was the only IFN-γ-responsive gene that was underexpressed more than 10-fold: *Ido1* mRNA expression was 29.4-fold greater ($p = 5 \times 10^{-22}$) in the lungs of W→W mice in comparison to W→K mice during week 9 postinfection.

To confirm these results with an unbiased set of genes, we performed whole-genome expression profiling on the lungs of infected chimeric mice. Of 41,171 genes analyzed, 1,761 were underexpressed and 1,894 genes were overexpressed in W→K mice compared to W→W mice during week 14 postinfection. A large fraction of the underexpressed genes are involved in immune cell recruitment, B cell and NK cell functions, and antigen presentation, whereas many of the overexpressed genes have roles in tissue remodeling and inflammation (Table 1). At 14 weeks postinfection, *Ido1* remained the most underexpressed gene in the lungs of W→K mice infected with *M. tuberculosis*; its mRNA in W→W mice was expressed at a level 36.6-fold higher than in the lungs of infected W→K mice ($p = 2.4 \times 10^{-22}$).

Differential Expression of *Ido1* in IFN-γR Chimeric Mice during *M. tuberculosis* Infection

To confirm the results obtained using whole-genome expression profiling by microarray, we first quantified the specific expression of *Ido1* mRNA by using quantitative real-time PCR during the course of TB infection.

Ido1 mRNA expression was detected at very low and similar amounts in the lungs of W→W and W→K mice after 2 weeks of infection with *M. tuberculosis* (Figure 4A). One week later, *Ido1* expression rose sharply in W→W mice and was maintained throughout the infection, mirroring the expression of *Ifng* mRNA in the lungs of these mice (Figure 4B). In contrast, *Ido1* expression was reduced by 95% in the lungs of mice whose nonhematopoietic cells are unable to respond to IFN-γ, even though the

Table 1. Selected Genes Under- or Overexpressed in the Lungs of W→K Mice Compared to W→W Mice 14 Weeks after Infection with *M. tuberculosis*

Name	Sequence Description	Accession Numbers	Fold Change	p Value
Stfa1	Stefin A1	NM_001001332	35.72946	3.00E-22
Glycam1	Glycosylation dependent cell adhesion molecule 1	NM_008134	28.69311	2.00E-20
Cxcl2	Chemokine (C-X-C motif) ligand 2	NM_009140	27.19208	6.00E-22
Camp	Cathelicidin antimicrobial peptide	NM_009921	16.35017	1.00E-20
Il17a	Interleukin 17A	NM_010552	14.32831	2.00E-20
Ccl3	Chemokine (C-C motif) ligand 3	NM_011337	8.84707	1.00E-18
Csf3	Colony stimulating factor 3 (granulocyte)	NM_009971	6.82582	7.00E-16
Il1r2	Interleukin 1 receptor, type II	NM_010555	6.37657	9.00E-17
Sele	Selectin, endothelial cell	NM_011345	5.48462	9.00E-14
Ccr1	Chemokine (C-C motif) receptor 1	NM_009912	4.77916	1.00E-06
Mmp9	Matrix metallopeptidase 9	NM_013599	3.95812	5.00E-34
Cxcl4	Chemokine (C-X-C motif) ligand 4	NM_019932	3.88045	7.00E-13
Cxcl5	Chemokine (C-X-C motif) ligand 5	NM_009141	3.76224	1.00E-12
Il23a	Interleukin 23, alpha subunit p19	NM_031252	3.74914	4.00E-06
Il1b	Interleukin 1 beta	NM_008361	3.39765	3.00E-27
Il17f	Interleukin 17F	NM_145856	2.71424	1.00E-02
Irak2	Interleukin-1 receptor-associated kinase 2	NM_172161	2.66109	5.00E-09
Tnf	Tumor necrosis factor	NM_013693	2.60488	3.00E-17
Il6	Interleukin 6	NM_031168	2.56139	9.00E-17
Cxcl1	Chemokine (C-X-C motif) ligand 1	NM_008176	2.37728	9.00E-08
Col15a1	Procollagen, type XV	NM_009928	2.37712	1.00E-07
Cd14	CD14 antigen	NM_009841	2.35198	1.00E-07
Edn1	Endothelin 1	NM_010104	2.29886	2.00E-07
Tlr6	Toll-like receptor 6	NM_011604	2.1796	9.00E-07
Tlr4	Toll-like receptor 4	NM_021297	2.05686	2.00E-10
Psmb9	Proteosome subunit, beta type 9	NM_013585	−2.01649	6.00E-06
Tbx21	T-box 21	NM_019507	−2.02845	5.00E-06
Nox1	NADPH oxidase 1	NM_172203	−2.04629	4.00E-01
Stat1	Signal transducer and activator of transcription 1	NM_009283	−2.07716	3.00E-06
Tap1	Transporter 1, ATP-binding cassette, subfamily B	NM_013683	−2.12481	2.00E-06
Stat2	Signal transducer and activator of transcription 2	NM_019963	−2.2154	6.00E-07
Card11	Caspase recruitment domain family, member 11	NM_175362	−2.22414	5.00E-07
Cxcr3	*Mus musculus* chemokine (C-X-C motif) receptor 3	NM_009910	−2.40445	7.00E-08
Lta	Lymphotoxin A	NM_010735	−2.41145	7.00E-15
Ccr6	Chemokine (C-C motif) receptor 6	NM_009835	−2.47999	3.00E-08
C2ta	Class II transactivator	NM_007575	−2.51527	2.00E-08
Ifngr1	Interferon gamma receptor 1	NM_010511	−2.63842	6.00E-09
Cd79a	CD79A antigen (immunoglobulin-associated alpha)	NM_007655	−2.73226	3.00E-06
Gata3	GATA binding protein 3	NM_008091	−2.73872	3.00E-09
Cd19	CD19 antigen	NM_009844	−2.88237	7.00E-10
Ighg	Immunoglobulin heavy chain (gamma polypeptide)	BC092269	−3.15632	8.00E-11
H2-DMb2	Histocompatibility 2, class II, locus Mb2	NM_010388	−3.18093	8.00E-11
Cd79b	CD79B antigen	NM_008339	−3.3018	3.00E-11
Igtp	Interferon gamma-induced GTPase	NM_018738	−3.44126	1.00E-11
Bank1	B cell scaffold protein with ankyrin repeats 1	NM_001033350	−4.1653	3.00E-05
Cr2	Complement receptor 2	NM_007758	−4.40919	8.00E-13
Klrb1c	Killer cell lectin-like receptor subfamily B member 1C	NM_008527	−4.87152	3.00E-14
Igj	Immunoglobulin joining chain	NM_152839	−5.08559	3.00E-15

Table 1. *Continued*

Name	Sequence Description	Accession Numbers	Fold Change	p Value
Il22	Interleukin 22	NM_016971	−5.74921	1.00E-06
Ido1	Indoleamine-pyrrole 2,3 dioxygenase 1	NM_008324	−36.59276	2.00E-22

Microarray analysis was conducted on pools of RNA from five mice per group, and the pools of each group were hybridized against each other. The results are expressed as the fold change in mRNA expression.

expression of *Ifng* increased similarly to that in W→W mice after week 3 of infection. These findings imply that IFN-γ induces *Ido1* expression by nonhematopoietic cells in the lungs during infection with *M. tuberculosis* and are consistent with reports that IFN-γ can induce *Ido1* expression in cultured fibroblasts (Pfefferkorn et al., 1986) and epithelial cells (Rapoza et al., 1991). We also confirmed that IFN-γ treatment of cultured murine NIH/3T3 fibroblasts induces expression of *Ido1* (Figure S5).

We confirmed the underexpression of IDO at the protein level by using immunohistochemistry. In the lungs of W→W mice during the chronic phase of TB, airway epithelial cells and vascular endothelial cells stained intensely with an antibody to murine IDO. In addition, IDO expression was detected in cells localized in granulomas that displayed the morphological characteristics of macrophages and/or dendritic cells (Figure 4C). In comparison, IDO staining in the lungs of W→K mice 15 weeks postinfection could only be detected in macrophages and/or dendritic cells in granulomas, without any staining of epithelial or endothelial cells (Figure 4C).

Taken together, these results provide strong evidence that IFN-γ-dependent expression of IDO in nonhematopoietic lung cells contributes substantially to the overall expression of IDO in the lungs of mice chronically infected with *M. tuberculosis*.

Mice with *Ifngr1*$^{-/-}$ Nonhematopoietic Cells Develop an Excessive IL-17 Response to *M. tuberculosis*

Whole-genome expression profiling of the lungs of chimeric mice chronically infected with *M. tuberculosis* also revealed overexpression of numerous genes involved in inflammation (Table 1). Because we observed an exuberant inflammatory response, including recruitment of neutrophils, during the chronic stage of infection of W→K mice, we characterized the expression of IL-17 in detail and analyzed the time course of *Il17a* expression in the lungs of *M. tuberculosis*-infected mice by using

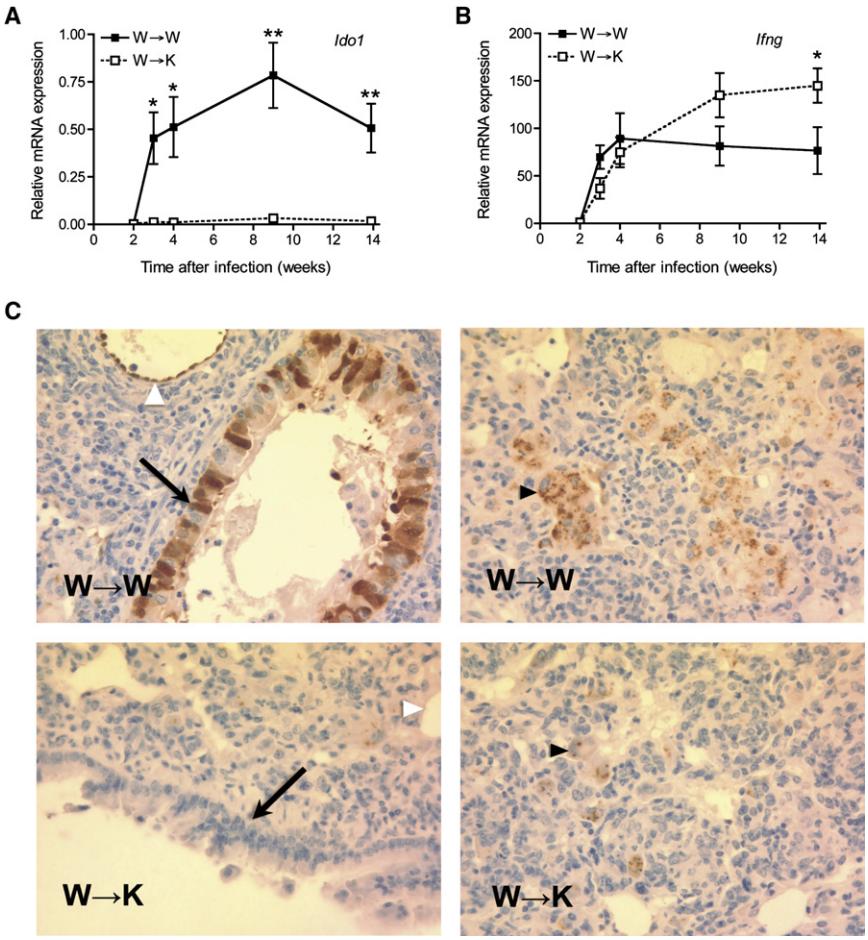


Figure 4. IFN-γ-Dependent Expression of IDO in Nonhematopoietic Cells Is Impaired in the Lungs of W→K Mice Infected with *M. tuberculosis*

(A and B) Quantitative real-time PCR (qRT-PCR) evaluation of *Ido1* (A) and *Ifng* (B) mRNA expression in the lungs of chimeric mice after infection with *M. tuberculosis*. Results are expressed as the average relative level of expression (±SE) of specific mRNA after normalization to 18S ribosomal RNA for four mice per time point and per group. Data were compared with a two-tailed Student's t test; *$p < 0.05$, **$p < 0.01$.

(C) Expression of IDO in lung sections of chimeric mice 15 weeks after infection with *M. tuberculosis*. Positive immunohistochemical staining in airway epithelial (arrows), vascular endothelial (white arrowheads), and myeloid (black arrowheads) cells. The image is shown at 400× the original magnification.

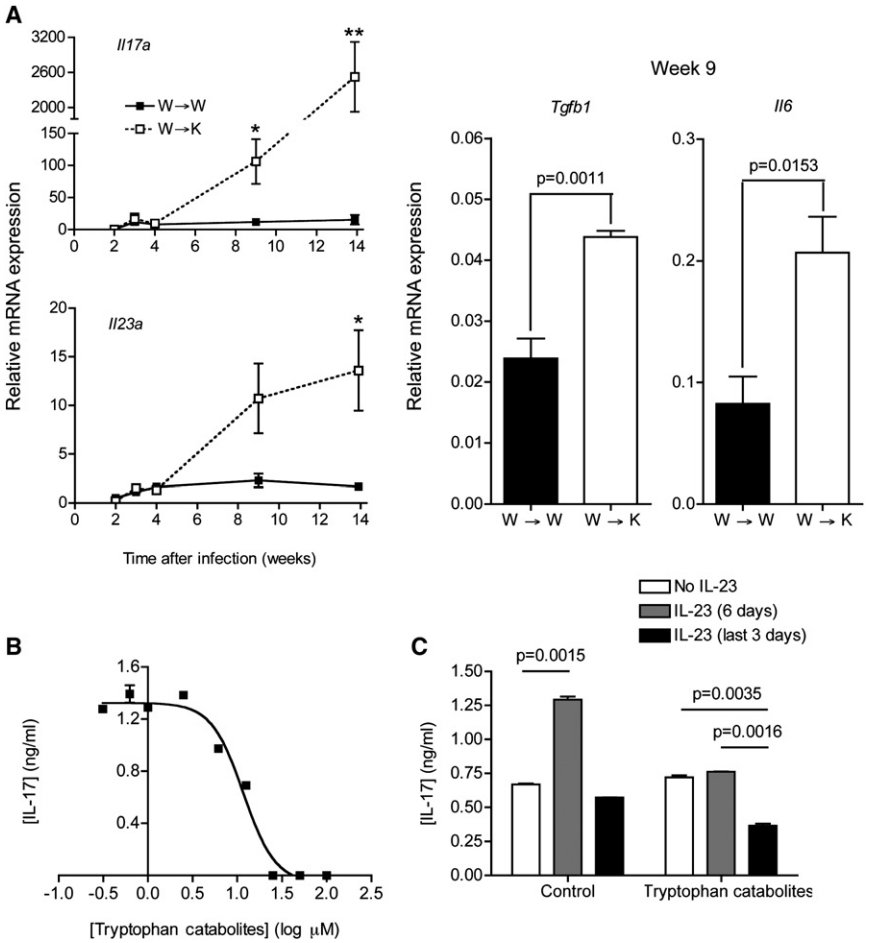


Figure 5. *Il17a* Expression during *M. tuberculosis* Infection In Vivo and Its Regulation by Kynurenines In Vitro

(A) qRT-PCR evaluation of *Il17a*, *Il23a*, *Tgfb1*, and *Il6* mRNA expression in the lungs of chimeric mice after infection with *M. tuberculosis*. Results are expressed as the average relative level of expression (±SE) of specific mRNA after normalization to 18S ribosomal RNA for four mice per time point and per group. *Il17a* and *Il23a* mRNA expression was quantitated 3, 4, 9, and 14 weeks after infection, and *Tgfb1* and *Il6* mRNA expression was assayed on samples harvested on week 9 postinfection. Data were compared with a two-tailed Student's t test; *$p < 0.05$, **$p < 0.01$ or indicated value.

(B) Dose response of IL-17 production by differentiating Th17 cells in vitro in the presence of increasing concentrations of tryptophan catabolites (L-kynurenine, 3′-hydroxy-DL-kynurenine, 3′-hydroxyanthranilic acid, anthranilic acid, and quinolinic acid). A nonlinear regression with variable slope analysis was applied with Prism software (GraphPad) so that an IC_{50} value of 11.7 ± 1.1 μM was determined.

(C) IL-17 production by differentiating Th17 cells in vitro in the presence of 15 μM of tryptophan catabolites after 6 days of culture, in the absence of IL-23 (white bars), in the presence of IL-23 for the last 3 days (gray bars), or for 6 days of culture (black bars).

Each condition was assayed in triplicate. The results are expressed as the mean concentration (±SE) of IL-17 in the culture supernatants after 6 days of incubation as measured by ELISA and are representative of two independent experiments.

quantitative real-time PCR. We also quantitated expression of genes involved in the generation or maintenance of IL-17-secreting cells, i.e., *Il6*, *Tgfb1*, and *Il23a* (Bettelli et al., 2007). The expression of *Il17a* mRNA in the lungs of W→W and W→K mice was low and equivalent until 4 weeks of infection with *M. tuberculosis* (Figure 5A). By week 9 postinfection, less than 2 weeks before the W→K mice started to die, *Il17a* expression increased more than 10-fold in the lungs of these mice but remained at the same low amount in W→W mice. By 14 weeks of infection, expression of *Il17a* in W→K mice was 163-fold higher than in W→W mice.

Role of Kynurenines in Regulating Development of Th17 Cells

Given that we observed marked underexpression of IDO in the lungs of infected W→K mice, and that IDO catabolizes tryptophan to products (collectively termed kynurenines) with immunoregulatory properties (Munn and Mellor, 2007), we determined whether defective generation of tryptophan catabolites might account for the overexpression of *Il17a* in the lungs. First, we examined the effects of tryptophan catabolites on the development of Th17 cells in vitro.

An equimolar solution of L-kynurenine, 3′-hydroxy-DL-kynurenine, 3′-hydroxyanthranilic acid, anthranilic acid, and quinolinic acid caused dose-dependent inhibition of IL-17 production by $CD4^+$ T cells under Th17 cell-differentiating conditions, which was detectable at a concentration of 7.5 μg/ml; complete inhibition was observed at a concentration of 25 μM for the mixture of tryptophan catabolites (Figure 5B). In these conditions, nonlinear regression analysis revealed an IC_{50} value of 11.7 ± 1.1 μM (10.4 ± 1.1 μg/ml). When these compounds were tested individually, 3′-hydroxyanthranilic acid was the most potent inhibitor of IL-17 production, with an IC_{50} of 27.7 ± 3.7 μM, followed by 3′-hydroxy-DL-kynurenine (IC_{50} = 68.1 ± 1.4 μM) and L-kynurenine (IC_{50} = 100.8 ± 1.0 μM) (Table 2). Anthranilic acid and quinolinic acid had no inhibitory effect within the range of concentrations assayed. The observation that the IC_{50} for the mixture is lower than for any of the individual compounds suggests that two or more of the individual compounds have distinct targets that affect Th17 cell differentiation and/or IL-17 secretion. We found that kynurenines were able to inhibit IFN-γ production during Th1 cell differentiation but required substantially higher concentrations (Table 2): the most potent inhibitor was 3′-hydroxyanthranilic acid, with an IC_{50} of 57.6 ± 1.0 μM. The combination of catabolites did not reduce further the production of IFN-γ (IC_{50} = 57.9 ± 1.3 μM); therefore, the combination of tryptophan catabolites was ~5-fold more potent for inhibition of Th17 versus Th1 cell differentiation. In light of our observation that W→K mice also exhibit poorer control of *M. tuberculosis* growth late in infection (Figure 1B), we examined

Table 2. 3′-Hydroxyanthranilic Acid Is the Most Potent Tryptophan Catabolite for the Inhibition of IL-17 Production by Th17 Cells In Vitro

	IC_{50} (μM)	
Tryptophan Metabolites	Th1 Cells	Th17 Cells
L-Kynurenine	154.5 ± 1.2	100.8 ± 1.0
3′-Hydroxy-DL-kynurenine	153.8 ± 1.1	68.1 ± 1.4
3′-Hydroxyanthranilic acid	57.6 ± 1.0	27.7 ± 3.7
Anthranilic acid	No inhibition	No inhibition
Quinolinic acid	111.5 ± 1.4	No inhibition
All	57.9 ± 1.3	11.7 ± 1.1

Inhibiting concentrations (IC_{50}) of L-kynurenine, 3′-hydroxy-DL-kynurenine, 3′-hydroxyanthranilic acid, anthranilic acid, or quinolinic acid on IFN-γ and IL-17 production by differentiating Th1 and Th17 cells in vitro, respectively. The results are expressed as the average IC_{50} values (±SE), calculated with a nonlinear regression with variable slope (Prism software, GraphPad).

kynurenines for the ability to inhibit growth of *M. tuberculosis* in vitro (Figure S5). Although we found that kynurenines inhibited growth of *M. tuberculosis* at concentrations previously reported to inhibit growth of *E. coli*, the effective concentrations were ~20-fold higher than the concentrations that inhibited Th17 cell differentiation.

Because we also observed that IL-23p19 was overexpressed in the lungs of *M. tuberculosis*-infected W→K mice, and because IL-23 promotes development and maintenance of Th17 cells in peripheral tissues as well as in lymph nodes (McGeachy et al., 2009), we tested the hypothesis that tryptophan catabolites inhibit the action of IL-23 during Th17 cell differentiation. We confirmed that IL-23 enhanced production of IL-17 under the conditions of our assay and found that tryptophan catabolites completely abrogated the effect of IL-23, even when they were only included during the latter stages of Th17 cell differentiation (Figure 5C). Taken together, these data indicate that low concentrations of kynurenines are capable of controlling the development of Th17 cells in vitro, in an IL-23-dependent fashion.

DISCUSSION

Whereas IFN-γ is essential for immune control of *M. tuberculosis*, its targets and functions are still incompletely understood. Because macrophages are a major cellular reservoir for *M. tuberculosis*, previous studies have focused on the effects of IFN-γ on these cells, and *Nos2* and *Irgm1* are the only two IFN-γ-dependent macrophage effector genes known to be essential for the control of tuberculosis (MacMicking et al., 1997; MacMicking et al., 2003).

In the studies reported here, we provide the first direct evidence that macrophages (and possibly other hematopoietic cells) must be able to respond to IFN-γ in vivo in order to control growth of *M. tuberculosis*. We also found that nonhematopoietic cells must be responsive to IFN-γ for durable control of bacterial growth and survival of the host. One of the mechanisms involving IFN-γ-responsive epithelial and endothelial cells is expression of IDO and regulation of IL-17 expression and neutrophilic inflammation in the lungs.

During the acute stage of infection, the adaptive immune response and its capacity to limit bacterial growth was unaffected by the absence of IFN-γR on nonhematopoietic cells. In accord with the observation that IFN-γ induces expression of CXCL9, CXCL10, and CXCL11 by cultured epithelial cells (Sauty et al., 1999), we observed a transient deficit in expression of these chemokines, but this had no effect on recruitment of T cells to the lungs in W→K mice. The earliest detectable difference between *M. tuberculosis*-infected W→K and W→W mice was a quantitative defect of lung myeloid dendritic cells and interstitial macrophages. This defect, detectable by week 3 post-infection, could explain the lower bacterial burden in W→K mice at that time, given that reduced recruitment of target cells, such as macrophages, can negatively influence the growth of mycobacteria (Davis and Ramakrishnan, 2009). However, by the ninth week of infection, the number of recruited macrophages and myeloid dendritic cells in the lungs was similar in both groups.

During the chronic stages of infection, W→K mice exhibited poorer control of bacterial growth, overexpression of IL-17, and neutrophilic inflammation in the lungs. These observations could have at least two potential general explanations. One is that nonhematopoietic cells are reservoirs of *M. tuberculosis*, and IFN-γ controls growth of bacteria in these cells. Despite in vitro data showing that *M. tuberculosis* can be taken up by cultured epithelial and endothelial cells (Bermudez and Goodman, 1996; Debbabi et al., 2005; Mehta et al., 2006), and some evidence that *M. tuberculosis* can be detected in lung epithelial cells in experimental infections (Rivas-Santiago et al., 2008; Teitelbaum et al., 1999), most evidence favors macrophages and dendritic cells as the cellular reservoirs for *M. tuberculosis* (Wolf et al., 2007). In our studies, acid-fast staining of the lungs of W→K mice indicated that most of the bacteria were associated with cells having the morphology of macrophages and/or dendritic cells, and at later stages of infection, bacteria were also associated with neutrophils. Therefore, the in vivo significance of nonhematopoietic cells as reservoirs of *M. tuberculosis* remains controversial and unlikely to explain our results. Consequently, any IFN-γ-inducible antimycobacterial activity provided by nonhematopoietic cells would probably act through secreted factors. Although nonhematopoietic cells can respond to *M. tuberculosis* by secreting TNF, GM-CSF, and MCP-1 (CCL2) (Lin et al., 1998) and they can produce antimicrobial products (Evans et al., 2009), few of these depend on IFN-γ, e.g., inducible nitric oxide synthase, β-defensins, NADPH oxidases, and IDO. Among those, we found that *Ido1* was the most underexpressed IFN-γ-responsive gene in W→K mice during chronic TB and that epithelial and endothelial cells were the major source of this enzyme at that time. IDO catalyzes the first step of the degradation of tryptophan and is induced by IFN-γ in a wide variety of cells (Carlin et al., 1989). Its antimicrobial activity was originally attributed to tryptophan depletion (Pfefferkorn, 1984); this is unlikely to account for our observations, given that *M. tuberculosis* can synthesize tryptophan (Parish and Stoker, 2002). More recent data indicate that tryptophan catabolites generated by IDO, or kynurenines, possess bacteriostatic activity (Narui et al., 2009), although we found that inhibition of *M. tuberculosis* required kynurenine

concentrations at least 20-fold greater than the concentrations that inhibit Th17 cell differentiation in vitro. Because macrophages and dendritic cells in both W→W and W→K mice can respond to IFN-γ and express IDO in vivo, it is unlikely that kynurenines mediate antimycobacterial activity strictly in an intracellular environment. Other IFN-γ-inducible molecules expressed in nonhematopoietic cells and with a potential role in bacteriostasis include inducible nitric oxide synthase (NOS2) and β-defensins. The expression profile of these genes did not suggest any involvement in the mortality of infected W→K mice. Lastly, expression of NADPH oxidase *Nox1*, also induced in nonhematopoietic cells by IFN-γ and implicated in control of bacterial infection (Leto and Geiszt, 2006; Robbins et al., 1994), was only moderately reduced in W→K mice. The importance of Nox1 in control of *M. tuberculosis* is unknown, but mice deficient in the related phagocyte NADPH oxidase Nox2 do not succumb to TB (Nathan and Shiloh, 2000).

The second general mechanism that may account for the death of W→K mice is dysregulation of the immune response during chronic infection. Although IL-10 contributes to regulation of immunity to TB during chronic infection (Higgins et al., 2009), we did not observe any defect in IL-10 expression in infected W→K mice. IDO has also been implicated in the regulation of immune responses in several contexts (Brandacher et al., 2008; Katz et al., 2008; Le and Broide, 2006; Zelante et al., 2009). Much attention has been focused on IDO in regulatory dendritic cells (Mellor and Munn, 2004) but nonhematopoietic cells from human lung have been reported to regulate T cell proliferation via IDO-dependent mechanisms in vitro (Heseler et al., 2008). In our studies, *Ido1* mRNA was detectable in the lungs throughout infection with *M. tuberculosis*. However, expression of the protein was limited to myeloid cells during the acute phase (data not shown). Maximum IDO expression appeared after 9 weeks of infection, in an IFN-γR-dependent fashion and in airway epithelial cells and vascular endothelial cells. This pattern suggests tissue-specific, posttranscriptional regulation and may explain why IDO is only required during later stages of infection. The observation that epithelial and endothelial cells in W→K mice did not express detectable amounts of IDO when IDO was readily detected in epithelial and endothelial cells of W→W mice provides strong evidence that these cells in the lungs were of recipient origin. This is consistent with the observation that bone marrow cells do not differentiate into lung epithelial cells at a detectable frequency (Kotton et al., 2005).

Other important observations in chronically infected chimeric mice were the dramatic increase in IL-17 expression, induction of CXCL2, and a massive influx of neutrophils in the lungs, starting at week 9 and peaking at week 14 of infection. The role of IL-17 on neutrophil recruitment has been extensively studied (Linden et al., 2005), but the relationship between *M. tuberculosis* infection and IL-17 has only been recently examined (Khader and Cooper, 2008). Most evidence to date has indicated a beneficial role for IL-17 in immunity to *M. tuberculosis*. In particular, IL-17 is required for a protective memory response after subunit vaccination (Khader et al., 2007). In addition, gene delivery of IL-23 positively influences the outcome of *M. tuberculosis* infection (Happel et al., 2005). One study showed that infection of *Ifng*$^{-/-}$ mice with BCG leads to increased frequency of IL-17-producing cells, but the investigators did not report the outcome of this imbalance in terms of pathology or bacterial control (Cruz et al., 2006). In our experiments, given the timing and the amplitude of the neutrophilic inflammation associated with the expression of IL-17 in infected W→K mice, it is likely that overexpression of IL-17 contributes to the death of W→K mice, through extensive tissue damage and impaired respiratory function. Unchecked Th17 cell responses have been associated with several inflammatory conditions. A murine model of the severe inflammation observed in chronic granulomatous disease (CGD) patients infected with *Aspergillus* revealed an excessive IL-17 response provoked by the impaired conversion of tryptophan into kynurenines (Romani et al., 2008). In accordance with this observation, we found that individual kynurenines have a direct and additive inhibitory effect on the development of Th17 cells in vitro, at concentrations found in vivo during viral pneumonia (Christen et al., 1990). This effect on Th17 cell differentiation was selective, and at least in part mediated by inhibition of the effects of IL-23; although kynurenines also inhibited Th1 differentiation, much higher concentrations were required.

We therefore propose a model in which *Ifngr1*$^{-/-}$ nonhematopoietic cells, unable to respond to IFNγ during the chronic phase of *M. tuberculosis* infection, fail to express the enzyme IDO and to convert tryptophan to kynurenines. The ongoing bacterial replication characterizing chronic TB in the murine model (Gill et al., 2009) provides sustained proinflammatory signals which, in the absence of kynurenines, triggers excessive production of IL-17 and lethal lung neutrophilia.

Because the human response to infection with *M. tuberculosis* can vary greatly, from asymptomatic latent infection to progressive lung destruction with formation of pulmonary cavities and extensive disability among survivors (de Valliere and Barker, 2004), evidence that defective expression of IDO in pulmonary parenchymal cells, with overexpression of IL-17 and excessive inflammation contributes to fatal infection in mice, provides an incentive to determine whether these mechanisms contribute to morbidity and mortality in humans with tuberculosis.

EXPERIMENTAL PROCEDURES

Mice

C57BL/6 congenic CD45.1^{+} wild-type (W) and CD45.2^{+} *Ifngr1*$^{-/-}$ (K) mice were originally purchased from The Jackson Laboratory (Bar Harbor, ME). They were bred as homozygotes and maintained under specific pathogen-free conditions at the New York University Medical Center (NYUMC, New York, NY). For infections with *Mycobacterium tuberculosis*, mice were housed under barrier conditions in the ABSL-3 facility at NYUMC. All mice used were females, between 8 and 12 weeks of age at the beginning of the experiment. For tissue harvest, mice were euthanized by CO_2 asphyxiation followed by cervical dislocation. All experiments were performed with the prior approval of NYUMC Institutional Animal Care and Use Committee.

Generation of Bone Marrow Chimeras

Donor wild-type and *Ifngr1*$^{-/-}$ mice were euthanized with CO_2 asphyxiation and cervical dislocation, and femurs and tibias were removed aseptically. Bone marrow was flushed with cold DMEM (Invitrogen), supplemented with 10% heat-inactivated FCS (Invitrogen) and 2 mM L-glutamine (Invitrogen). Cells were washed twice with PBS without calcium and magnesium (Invitrogen), supplemented with 1% FCS. The suspension was depleted of mature T cells by treatment with microbeads coated with anti-Thy1.2 antibody (Miltenyi Biotec) followed by magnetic-activated cell sorting according to the

manufacturer's recommendations. Viable cells were counted in a hemacytometer with a Trypan blue exclusion assay. Recipient wild-type and *Ifngr1*$^{-/-}$ mice were irradiated with 10 Gy in split doses at 2 hr intervals. They were reconstituted no later than 6 hr after the last irradiation with 2 × 10^6 wild-type (W→W and W→K mice) or *Ifngr1*$^{-/-}$ (K→W and K→K mice) cells by intravenous injection. Mice were given sulfamethoxazole (150 mg/ml) and trimethoprim (30 mg/ml) in drinking water for the first 3 weeks of reconstitution. Chimeras were used no earlier than 6 weeks after transplantation. Prior to infection with *M. tuberculosis*, we confirmed that mice reconstituted with congenic bone marrow stem cells had achieved a satisfactory level of chimerism by assessing the number of CD45.1$^+$ (wild-type) and CD45.2$^+$ (*Ifngr1*$^{-/-}$) leukocytes in the lungs, using flow cytometry (Figure S1). In this organ, the proportion of donor-derived leukocytes averaged 86.6% ± 1% over multiple experiments, after the transfer of either wild-type or *Ifngr1*$^{-/-}$ marrow, and did not vary over time after *M. tuberculosis* infection. The same result was found in the spleen (data not shown).

Bacterial Infection

The H37Rv strain of *Mycobacterium tuberculosis* was grown as previously described (Banaiee et al., 2006). Chimeras were infected via the aerosol route, with an inhalation exposure system (Glas-Col) (Wolf et al., 2007), calibrated to deliver 150 colony-forming units (CFUs) per animal. The infectious dose was confirmed on day 1 by plating whole-lung homogenates from 5 sentinel mice on Middlebrook 7H11 agar. CFU were counted after incubation at 37°C for 2–3 weeks. To determine the bacterial load throughout the infection, we harvested the right lung, MLN, and spleen from chimeric mice, homogenized them and plated serial dilutions on Middlebrook 7H11 agar.

Histology and Immunohistochemistry

The left lung was excised, fixed in 4% paraformaldehyde (PFA) for 1 week at room temperature, and embedded in paraffin. Sections of 5 μm were cut and stained with hematoxylin and eosin. Alternatively, sections were treated with an acid-fast Kinyoun's stain to reveal the presence of *M. tuberculosis* and counterstained with Brilliant Green.

For indoleamine 2,3-deoxygenase (IDO) immunostaining, PFA-fixed, paraffin-embedded lung sections were deparaffinized with CitriSolv solution (Fisher Scientific) and rehydrated by successive baths of decreasing ethanol concentration. Endogenous peroxidase activity was blocked by treatment with 3% H_2O_2. Endogenous avidin/biotin activity was blocked with a commercially available kit (Vector Laboratories). Nonspecific binding sites were saturated by a solution of bovine serum albumin 2%. IDO was stained with a polyclonal rabbit anti-murine IDO antibody (Alexis Biochemicals). Subsequently, the sections were incubated with biotinylated polyclonal goat anti-rabbit IgG, streptavidin-conjugated horseradish peroxidase and DAB chromogenic substrate (Vector Laboratories). The tissues were counterstained with hematoxylin, dehydrated, and mounted with PerMount solution (Fisher Scientific).

Cell Isolation and Flow Cytometry

The right lung as well as the MLN were removed and processed for flow cytometry as previously described (Wolf et al., 2007). Antibodies conjugated to various fluorophores and directed against the following surface markers were used: CD4 (RM4-5, BioLegend), CD8α (53-6.7, BD Biosciences), CD62L (MEL-14, BioLegend), CD45RA (14.8, BioLegend), Dx5 (BD Biosciences), B220 (RA3-6B2, BD Biosciences), CD19 (6D5, BioLegend), CD11c (HL3, BD Biosciences), CD11b (M1/70, BD Biosciences), Gr-1 (RB6-8C5, BD Biosciences), and CD45.2 (104, BD Biosciences) A minimum of 200,000 events per sample, gated on live cells with forward and side scatter parameters, was acquired with an LSRII and the FACSDiva software (BD Biosciences). Data were analyzed with the FlowJo software (TreeStar).

Microarray Analysis

Total RNA was extracted from the left lung with TriZol reagent (Invitrogen) and was processed as previously described for removal of contaminating genomic DNA and reverse transcription (Banaiee et al., 2006). RNA integrity of individual samples was confirmed by ribosomal RNA profiles at the Genomics Facility of the Cancer Institute of NYU Langone Medical Center. RNA samples of each group of mice were pooled and the resulting pools were hybridized against each other for differential gene expression analysis with Agilent Whole Mouse Genome Oligo Microarray (Miltenyi Biotec). Microarray data are available from the National Center for Biotechnology Information Gene Expression Omnibus (NCBI-GEO) database under accession number GSE19148.

Real-Time Quantitative RT-PCR

Total RNA was extracted from lung tissues as described above. The cDNA equivalent of 50 ng of total RNA was analyzed for specific gene expression in triplicate for each sample by quantitative real-time PCR with Platinum SYBR Green qPCR SuperMix (Invitrogen) on an MJ Research Opticon 2. Sequences of the primer pairs can be found in Table S1. Thermal cycling conditions were 95°C for 10 min then 40 cycles at 94°C for 45 s, 58°C for 30 s, and 72°C for 30 s. For quantitation, the relative values were determined by comparing the threshold cycle C(t) of each sample to a standard curve consisting of serial dilutions of a positive control cDNA sample. Results were normalized with 18S rRNA expression as an internal standard for each sample.

Cell Culture and Inhibition Studies

For the in vitro differentiation of Th17 cells, CD4$^+$ T cells were isolated from spleen and lymph nodes of C57BL/6 mice followed by magnetic cell sorting using anti-CD4$^+$ antibody-coated microbeads (Miltenyi Biotec). Cells were resuspended in RPMI supplemented with 10% FBS, hamster anti-murine CD3 antibody (0.25 μg/ml), hamster anti-murine CD28 antibody (1 μg/ml), anti-murine IL-4 neutralizing antibody (1 μg/ml), anti-murine IFN-γ neutralizing antibody (1 μg/ml), recombinant murine IL-6 (20 ng/ml, PeproTech), recombinant human TGFβ (0.5 μg/ml, PeproTech), and recombinant murine IL-23 (20 ng/ml, eBioscience). All antibodies were purchased from BioLegend. The cells were seeded at a density of 10^5 cells/well in 96-well plates precoated with 0.12 μg/ml of goat anti-hamster IgG antibody (Vector Laboratories) and cultured for 6 days at 37°C in 5% CO_2. In some experiments, IL-23 was omitted or only added on the third day of culture. The concentration of IL-17 in culture supernatants was measured by ELISA (R&D Systems).

For comparison studies with Th1 cells, T cells were differentiated in the same in vitro conditions, with only anti-murine IL-4 neutralizing antibody, recombinant murine IL-2 (10 ng/ml, eBioscience), and recombinant murine IL-12p70 (20 ng/ml, BD Biosciences) and CD3/CD28 stimulation. The concentration of IFN-γ in culture supernatants was measured by ELISA (BD Biosciences).

L-kynurenine, 3′-hydroxy-DL-kynurenine, 3′-hydroxyanthranilic acid, anthranilic acid, and quinolinic acid (Sigma) were dissolved in RPMI medium under agitation at 1 mM concentration and sterile filtered. Tryptophan catabolites were added individually or in combination, in 2-fold dilutions, to the differentiating medium of Th1 or Th17 cells for the 6 days of culture.

Statistical Analysis

Results are expressed as mean and standard error. Student's two-tailed t test was used for comparing experimental groups, unless otherwise stated, with $p < 0.05$ considered significant.

SUPPLEMENTAL DATA

Supplemental Data include five figures and one table and can be found with this article online at http://www.cell.com/immunity/supplemental/S1074-7613(09)00509-3.

ACKNOWLEDGMENTS

We thank J. LaFaille for invaluable assistance in making these studies possible and for helpful comments on the manuscript. We also thank E. Allen, E. Hayes, and S. Stukes for expert technical assistance. This work was supported by NIH grants R03 AI053074 and R01 AI059667.

Received: May 11, 2009
Revised: July 21, 2009
Accepted: October 6, 2009
Published online: December 17, 2009

REFERENCES

Banaiee, N., Kincaid, E.Z., Buchwald, U., Jacobs, W.R., Jr., and Ernst, J.D. (2006). Potent inhibition of macrophage responses to IFN-gamma by live virulent Mycobacterium tuberculosis is independent of mature mycobacterial lipoproteins but dependent on TLR2. J. Immunol. *176*, 3019–3027.

Bermudez, L.E., and Goodman, J. (1996). Mycobacterium tuberculosis invades and replicates within type II alveolar cells. Infect. Immun. *64*, 1400–1406.

Bettelli, E., Oukka, M., and Kuchroo, V.K. (2007). T(H)-17 cells in the circle of immunity and autoimmunity. Nat. Immunol. *8*, 345–350.

Brandacher, G., Margreiter, R., and Fuchs, D. (2008). Clinical relevance of indoleamine 2,3-dioxygenase for alloimmunity and transplantation. Curr. Opin. Organ Transplant. *13*, 10–15.

Carlin, J.M., Ozaki, Y., Byrne, G.I., Brown, R.R., and Borden, E.C. (1989). Interferons and indoleamine 2,3-dioxygenase: role in antimicrobial and antitumor effects. Experientia *45*, 535–541.

Christen, S., Peterhans, E., and Stocker, R. (1990). Antioxidant activities of some tryptophan metabolites: possible implication for inflammatory diseases. Proc. Natl. Acad. Sci. USA *87*, 2506–2510.

Cooper, A.M., Dalton, D.K., Stewart, T.A., Griffin, J.P., Russell, D.G., and Orme, I.M. (1993). Disseminated tuberculosis in interferon gamma gene-disrupted mice. J. Exp. Med. *178*, 2243–2247.

Cruz, A., Khader, S.A., Torrado, E., Fraga, A., Pearl, J.E., Pedrosa, J., Cooper, A.M., and Castro, A.G. (2006). Cutting edge: IFN-gamma regulates the induction and expansion of IL-17-producing CD4 T cells during mycobacterial infection. J. Immunol. *177*, 1416–1420.

Davis, J.M., and Ramakrishnan, L. (2009). The role of the granuloma in expansion and dissemination of early tuberculous infection. Cell *136*, 37–49.

de Valliere, S., and Barker, R.D. (2004). Residual lung damage after completion of treatment for multidrug-resistant tuberculosis. Int. J. Tuberc. Lung Dis. *8*, 767–771.

Debbabi, H., Ghosh, S., Kamath, A.B., Alt, J., Demello, D.E., Dunsmore, S., and Behar, S.M. (2005). Primary type II alveolar epithelial cells present microbial antigens to antigen-specific CD4+ T cells. Am. J. Physiol. Lung Cell. Mol. Physiol. *289*, L274–L279.

Ehrt, S., Schnappinger, D., Bekiranov, S., Drenkow, J., Shi, S., Gingeras, T.R., Gaasterland, T., Schoolnik, G., and Nathan, C. (2001). Reprogramming of the macrophage transcriptome in response to interferon-gamma and Mycobacterium tuberculosis: signaling roles of nitric oxide synthase-2 and phagocyte oxidase. J. Exp. Med. *194*, 1123–1140.

Evans, S.E., Scott, B.L., Clement, C.G., Larson, D.T., Kontoyiannis, D., Lewis, R.E., Lasala, P.R., Pawlik, J., Peterson, J.W., Chopra, A.K., et al. (2009). Stimulated Innate Resistance of Lung Epithelium Protects Mice Broadly Against Bacteria and Fungi. Am. J. Respir. Cell Mol. Biol., in press. Published online March 27, 2009. 10.1165/rcmb.2008-0260OC.

Fieschi, C., Dupuis, S., Catherinot, E., Feinberg, J., Bustamante, J., Breiman, A., Altare, F., Baretto, R., Le Deist, F., Kayal, S., et al. (2003). Low penetrance, broad resistance, and favorable outcome of interleukin 12 receptor beta1 deficiency: medical and immunological implications. J. Exp. Med. *197*, 527–535.

Filipe-Santos, O., Bustamante, J., Chapgier, A., Vogt, G., de Beaucoudrey, L., Feinberg, J., Jouanguy, E., Boisson-Dupuis, S., Fieschi, C., Picard, C., and Casanova, J.L. (2006). Inborn errors of IL-12/23- and IFN-gamma-mediated immunity: molecular, cellular, and clinical features. Semin. Immunol. *18*, 347–361.

Flynn, J.L., Chan, J., Triebold, K.J., Dalton, D.K., Stewart, T.A., and Bloom, B.R. (1993). An essential role for interferon gamma in resistance to Mycobacterium tuberculosis infection. J. Exp. Med. *178*, 2249–2254.

Gill, W.P., Harik, N.S., Whiddon, M.R., Liao, R.P., Mittler, J.E., and Sherman, D.R. (2009). A replication clock for Mycobacterium tuberculosis. Nat. Med. *15*, 211–214.

Gonzalez-Juarrero, M., Shim, T.S., Kipnis, A., Junqueira-Kipnis, A.P., and Orme, I.M. (2003). Dynamics of macrophage cell populations during murine pulmonary tuberculosis. J. Immunol. *171*, 3128–3135.

Gutierrez, M.G., Master, S.S., Singh, S.B., Taylor, G.A., Colombo, M.I., and Deretic, V. (2004). Autophagy is a defense mechanism inhibiting BCG and Mycobacterium tuberculosis survival in infected macrophages. Cell *119*, 753–766.

Happel, K.I., Lockhart, E.A., Mason, C.M., Porretta, E., Keoshkerian, E., Odden, A.R., Nelson, S., and Ramsay, A.J. (2005). Pulmonary interleukin-23 gene delivery increases local T-cell immunity and controls growth of Mycobacterium tuberculosis in the lungs. Infect. Immun. *73*, 5782–5788.

Heseler, K., Spekker, K., Schmidt, S.K., MacKenzie, C.R., and Daubener, W. (2008). Antimicrobial and immunoregulatory effects mediated by human lung cells: role of IFN-gamma-induced tryptophan degradation. FEMS Immunol. Med. Microbiol. *52*, 273–281.

Higgins, D.M., Sanchez-Campillo, J., Rosas-Taraco, A.G., Lee, E.J., Orme, I.M., and Gonzalez-Juarrero, M. (2009). Lack of IL-10 alters inflammatory and immune responses during pulmonary Mycobacterium tuberculosis infection. Tuberculosis (Edinb.) *89*, 149–157.

Jouanguy, E., Lamhamedi-Cherradi, S., Altare, F., Fondaneche, M.C., Tuerlinckx, D., Blanche, S., Emile, J.F., Gaillard, J.L., Schreiber, R., Levin, M., et al. (1997). Partial interferon-gamma receptor 1 deficiency in a child with tuberculoid bacillus Calmette-Guerin infection and a sibling with clinical tuberculosis. J. Clin. Invest. *100*, 2658–2664.

Katz, J.B., Muller, A.J., and Prendergast, G.C. (2008). Indoleamine 2,3-dioxygenase in T-cell tolerance and tumoral immune escape. Immunol. Rev. *222*, 206–221.

Khader, S.A., and Cooper, A.M. (2008). IL-23 and IL-17 in tuberculosis. Cytokine *41*, 79–83.

Khader, S.A., Bell, G.K., Pearl, J.E., Fountain, J.J., Rangel-Moreno, J., Cilley, G.E., Shen, F., Eaton, S.M., Gaffen, S.L., Swain, S.L., et al. (2007). IL-23 and IL-17 in the establishment of protective pulmonary CD4+ T cell responses after vaccination and during Mycobacterium tuberculosis challenge. Nat. Immunol. *8*, 369–377.

Kotton, D.N., Fabian, A.J., and Mulligan, R.C. (2005). Failure of bone marrow to reconstitute lung epithelium. Am. J. Respir. Cell Mol. Biol. *33*, 328–334.

Le, A.V., and Broide, D.H. (2006). Indoleamine-2,3-dioxygenase modulation of allergic immune responses. Curr. Allergy Asthma Rep. *6*, 27–31.

Leto, T.L., and Geiszt, M. (2006). Role of Nox family NADPH oxidases in host defense. Antioxid. Redox Signal. *8*, 1549–1561.

Lin, Y., Zhang, M., and Barnes, P.F. (1998). Chemokine production by a human alveolar epithelial cell line in response to Mycobacterium tuberculosis. Infect. Immun. *66*, 1121–1126.

Linden, A., Laan, M., and Anderson, G.P. (2005). Neutrophils, interleukin-17A and lung disease. Eur. Respir. J. *25*, 159–172.

MacMicking, J.D., North, R.J., LaCourse, R., Mudgett, J.S., Shah, S.K., and Nathan, C.F. (1997). Identification of nitric oxide synthase as a protective locus against tuberculosis. Proc. Natl. Acad. Sci. USA *94*, 5243–5248.

MacMicking, J.D., Taylor, G.A., and McKinney, J.D. (2003). Immune control of tuberculosis by IFN-gamma-inducible LRG-47. Science *302*, 654–659.

McGeachy, M.J., Chen, Y., Tato, C.M., Laurence, A., Joyce-Shaikh, B., Blumenschein, W.M., McClanahan, T.K., O'Shea, J.J., and Cua, D.J. (2009). The interleukin 23 receptor is essential for the terminal differentiation of interleukin 17-producing effector T helper cells in vivo. Nat. Immunol. *10*, 314–324.

Mehta, P.K., Karls, R.K., White, E.H., Ades, E.W., and Quinn, F.D. (2006). Entry and intracellular replication of Mycobacterium tuberculosis in cultured human microvascular endothelial cells. Microb. Pathog. *41*, 119–124.

Mellor, A.L., and Munn, D.H. (2004). IDO expression by dendritic cells: tolerance and tryptophan catabolism. Nat. Rev. Immunol. *4*, 762–774.

Munn, D.H., and Mellor, A.L. (2007). Indoleamine 2,3-dioxygenase and tumor-induced tolerance. J. Clin. Invest. *117*, 1147–1154.

Nagabhushanam, V., Solache, A., Ting, L.M., Escaron, C.J., Zhang, J.Y., and Ernst, J.D. (2003). Innate inhibition of adaptive immunity: Mycobacterium tuberculosis-induced IL-6 inhibits macrophage responses to IFN-gamma. J. Immunol. *171*, 4750–4757.

Narui, K., Noguchi, N., Saito, A., Kakimi, K., Motomura, N., Kubo, K., Takamoto, S., and Sasatsu, M. (2009). Anti-infectious activity of tryptophan

metabolites in the L-tryptophan-L-kynurenine pathway. Biol. Pharm. Bull. *32*, 41–44.

Nathan, C., and Shiloh, M.U. (2000). Reactive oxygen and nitrogen intermediates in the relationship between mammalian hosts and microbial pathogens. Proc. Natl. Acad. Sci. USA *97*, 8841–8848.

Parish, T., and Stoker, N.G. (2002). The common aromatic amino acid biosynthesis pathway is essential in Mycobacterium tuberculosis. Microbiology *148*, 3069–3077.

Pfefferkorn, E.R. (1984). Interferon gamma blocks the growth of Toxoplasma gondii in human fibroblasts by inducing the host cells to degrade tryptophan. Proc. Natl. Acad. Sci. USA *81*, 908–912.

Pfefferkorn, E.R., Rebhun, S., and Eckel, M. (1986). Characterization of an indoleamine 2,3-dioxygenase induced by gamma-interferon in cultured human fibroblasts. J. Interferon Res. *6*, 267–279.

Rapoza, P.A., Tahija, S.G., Carlin, J.P., Miller, S.L., Padilla, M.L., and Byrne, G.I. (1991). Effect of interferon on a primary conjunctival epithelial cell model of trachoma. Invest. Ophthalmol. Vis. Sci. *32*, 2919–2923.

Rivas-Santiago, B., Contreras, J.C., Sada, E., and Hernandez-Pando, R. (2008). The potential role of lung epithelial cells and beta-defensins in experimental latent tuberculosis. Scand. J. Immunol. *67*, 448–452.

Robbins, R.A., Springall, D.R., Warren, J.B., Kwon, O.J., Buttery, L.D., Wilson, A.J., Adcock, I.M., Riveros-Moreno, V., Moncada, S., Polak, J., et al. (1994). Inducible nitric oxide synthase is increased in murine lung epithelial cells by cytokine stimulation. Biochem. Biophys. Res. Commun. *198*, 835–843.

Romani, L., Fallarino, F., De Luca, A., Montagnoli, C., D'Angelo, C., Zelante, T., Vacca, C., Bistoni, F., Fioretti, M.C., Grohmann, U., et al. (2008). Defective tryptophan catabolism underlies inflammation in mouse chronic granulomatous disease. Nature *451*, 211–215.

Sana, T.R., Janatpour, M.J., Sathe, M., McEvoy, L.M., and McClanahan, T.K. (2005). Microarray analysis of primary endothelial cells challenged with different inflammatory and immune cytokines. Cytokine *29*, 256–269.

Sauty, A., Dziejman, M., Taha, R.A., Iarossi, A.S., Neote, K., Garcia-Zepeda, E.A., Hamid, Q., and Luster, A.D. (1999). The T cell-specific CXC chemokines IP-10, Mig, and I-TAC are expressed by activated human bronchial epithelial cells. J. Immunol. *162*, 3549–3558.

Schaible, U.E., Sturgill-Koszycki, S., Schlesinger, P.H., and Russell, D.G. (1998). Cytokine activation leads to acidification and increases maturation of Mycobacterium avium-containing phagosomes in murine macrophages. J. Immunol. *160*, 1290–1296.

Schroder, K., Hertzog, P.J., Ravasi, T., and Hume, D.A. (2004). Interferon-gamma: an overview of signals, mechanisms and functions. J. Leukoc. Biol. *75*, 163–189.

Skold, M., and Behar, S.M. (2008). Tuberculosis triggers a tissue-dependent program of differentiation and acquisition of effector functions by circulating monocytes. J. Immunol. *181*, 6349–6360.

Teitelbaum, R., Schubert, W., Gunther, L., Kress, Y., Macaluso, F., Pollard, J.W., McMurray, D.N., and Bloom, B.R. (1999). The M cell as a portal of entry to the lung for the bacterial pathogen Mycobacterium tuberculosis. Immunity *10*, 641–650.

Ting, L.M., Kim, A.C., Cattamanchi, A., and Ernst, J.D. (1999). Mycobacterium tuberculosis inhibits IFN-gamma transcriptional responses without inhibiting activation of STAT1. J. Immunol. *163*, 3898–3906.

Wolf, A.J., Linas, B., Trevejo-Nunez, G.J., Kincaid, E., Tamura, T., Takatsu, K., and Ernst, J.D. (2007). Mycobacterium tuberculosis infects dendritic cells with high frequency and impairs their function in vivo. J. Immunol. *179*, 2509–2519.

Wolf, A.J., Desvignes, L., Linas, B., Banaiee, N., Tamura, T., Takatsu, K., and Ernst, J.D. (2008). Initiation of the adaptive immune response to Mycobacterium tuberculosis depends on antigen production in the local lymph node, not the lungs. J. Exp. Med. *205*, 105–115.

Yap, G.S., and Sher, A. (1999). Effector cells of both nonhemopoietic and hemopoietic origin are required for interferon (IFN)-gamma- and tumor necrosis factor (TNF)-alpha-dependent host resistance to the intracellular pathogen, Toxoplasma gondii. J. Exp. Med. *189*, 1083–1092.

Zelante, T., Fallarino, F., Bistoni, F., Puccetti, P., and Romani, L. (2009). Indoleamine 2,3-dioxygenase in infection: the paradox of an evasive strategy that benefits the host. Microbes Infect. *11*, 133–141.